European Review for Medical and Pharmacological Sciences 2021; 25: 3083-3096

Silver nanoparticles green synthesis *via cyanobacterium Phormidium* sp.: characterization, wound healing, antioxidant, antibacterial, and anti-inflammatory activities

N.S. YOUNIS[1,2], N.A. EL SEMARY[3,4], M.E. MOHAMED[1,5]

[1]Department of Pharmaceutical Sciences, College of Clinical Pharmacy, King Faisal University, Al-Ahsa, Saudi Arabia
[2]Pharmacology Department, Zagazig University, Zagazig, Egypt
[3]Biological Sciences Department, College of Science, King Faisal University, Al-Ahsa, Saudi Arabia
[4]Botany and Micrrobiology Department, Faculty of Sciences, Helwan University, Cairo, Egypt
[5]Department of Pharmacognosy, College of Pharmacy, Zagazig University, Zagazig, Egypt

Abstract. – OBJECTIVE: Green synthesis of silver nanoparticles (AgNPs) using cyanobacterial platforms is becoming more popular nowadays. In this study, the filamentous non-heterocystous *cyanobacterium Phormidium* sp. was used for AgNPs production. Then, it was investigated for its antibacterial and wound-healing properties.

MATERIALS AND METHODS: The *cyanobacterium* cultures were challenged by $AgNO_3$, and the obtained nanoparticles were characterized using UV and FTIR spectrometric methods. The antimicrobial activity of AgNPs was scrutinized against MRSA either alone or in combination 0.5% chloramphenicol. The green synthesized AgNPs were tested for their skin wound healing activity using several wound models at different concentrations.

RESULTS: The cyanobacterial culture extract showed the characteristic surface plasmon resonance peak at 440 nm for AgNPs. Different functional groups that could contribute to the reduction of Ag^+ to AgNPs or the stabilization of the nanoparticles were identified by the FTIR. AgNPs potentiated the antimicrobial activity of chloramphenicol against MRSA. Green synthesized silver nanoparticles have demonstrated topical effectiveness in different wound models, including excision, incision, and burn. Significant wound improvement and the increase in wound closure rate, hydroxyproline content, and the reduction in epithelialization period confirmed the wound healing potency of AgNPs. The enzymatic antioxidant level escalation and inflammatory cytokines attenuation supported the AgNPs substantial effect on wound repairing.

CONCLUSIONS: Biogenic AgNPs produced by *Phormidium* sp. showed significant antimicrobial together with wound healing abilities.

Key Words:
Anti-inflammatory, Antioxidant, *Cyanobacteria*, MRSA, Silver nanoparticles, Wound healing.

Introduction

Skin is the protective barrier that can distinguish, differentiate, and incorporate numerous indicators within the environment and instantly establish appropriate responses[1,2]. There are various types of wounds, including an incised, lacerated, abrasion, contusion, ulcer, and burn wounds [3]. The wound healing process involves four overlapping biological segments of hemostasis, inflammation, proliferation, and remodeling[1,4]. Irregularities or vascular obstruction in any of these phases may result in a long-lasting or deferred wound healing process leading to poorly healed skin tissue[1,4]. During the inflammatory phase (first 2-4 days of healing), inflammatory cells (neutrophils and macrophages) eliminate injured tissue and provide protection from infection and release chemotactic and mitogenic factors[4-6]. Throughout the proliferative phase, surrounding tissue fibroblasts proliferate to produce collagen, and concurrently epithelialization and angiogenesis arise[4]. Finally, during the remodeling phase, the newly produced collagen cross-links with the already existing collagen and protein molecules to intensify the scar tensile strength[2,4].

Nanoparticles are classified into organic and inorganic. Carbon nanoparticles represent the organic nanoparticles, while magnetic nanoparti-

Corresponding Author: Nancy S. Younis, MD; e-mail: nyounis@kfu.edu.sa, nancysafwet@hotmail.com

cles, noble metal nanoparticles (platinum, gold, and silver), and semiconductor nanoparticles (titanium dioxide and zinc oxide) exemplify the inorganic group. Inorganic nanoparticles are increasingly used in drug delivery due to their distinctive features such as ease of use, good functionality, biocompatibility, ability to target specific cells and control release of drugs[7].

Wound treatment products, widely referred to as 'colloidal silver', include solutions that contain various concentrations of ionic silver compounds[5]. The unique properties of silver nanoparticles (AgNPs) with a particle size between 1 nm and 100 nm, making them ideal for numerous technologies, including biomedical, optical, and antimicrobial applications[5]. Utilizing nanotechnology development, many novel therapeutics have been developed using nanomaterials depending on their unique chemical features. However, chemically-synthesized nanomaterials used in therapies contain traces of chemical allergens, which have brought about some health problems, including allergies, rashes, itching, and swelling[5].

Cyanobacteria represent an eco-friendly producer for biogenic nanoparticles. They possess the ability to biosynthesize nanoparticles, from the vicinity of ions and radionuclides in their niches as a part of mechanisms that help the organism to detoxify its environment[8]. Some cyanobacteria, such as *Plectonema boryanum*, demonstrated a potential to biotransform Au^{3+} to Au^{0} and subsequently the formation of gold nanoparticles (AuNPs)[9]. Cyanobacteria gained much intention as a noble metal nanoparticle producer as it is easy to grow and manipulate on relatively inexpensive growth media, which enables cost-effective production of these green nanoparticles.

Therefore, the present study focused on the biosynthesis and characterization of AgNPs produced by the filamentous, non-heterocystous *cyanobacterium Phormidium* sp. Furthermore, the wound healing effect of the produced AgNPs on different types of wounds, including excision, incision, and burn wounds, was investigated.

Materials and Methods

Cyanobacteria Culture

The *Phormidium* sp. was previously collected and purified from Alhasa, Eastern province, Kingdom of Saudi Arabia, in 2017[10].

Preparation of Silver Nitrate

A stock solution of silver nitrate (Sigma-Aldrich, St. Louis, MO, USA) of 1 M concentration was prepared and used in the study. The solution was kept in a dark bottle. For the synthesis of biogenic AgNPs, 5 ml of culture suspended in distilled water was completed to 19 ml by 0.1 M phosphate buffer at pH 7, and then 1 ml silver nitrate solutions of the concentration 0.5 mM) The reaction mixture was incubated at room temperature.

Silver Nanoparticles Synthesis

Production of AgNPs from *Phormidium* sp. was based on the method described by Hamouda et al [11] with some modifications. Mid-logarithmic *Phormidium* sp. culture was grown for 60 days in F_2 medium, the cells were harvested by centrifugation (10 minutes, 2000 x g), and 15 mg of the biomass was suspended in phosphate buffer (pH 7) (19 ml) the 1 ml of 0.5 mM of silver nitrate ($AgNO_3$) was added. The cultures were kept under illumination (2000 ± 200 Lux) for 72 hours. A negative control was prepared by repeating the above process and replacing cyanobacterial biomass with distilled water. Turning the external solution into yellow then brown indicated the production of silver nanoparticles. The process of AgNPs production was monitored by UV-Vis spectrometry (Genesys10S, Thermo Scientific, Austin, TX, USA) scan every 6 hours.

Characterization of the Produced Biogenic AgNPs

Characterization of silver nanoparticles was performed using UV-Vis spectrometry scan as mentioned above in the range of 200-900 nm. In addition, Fourier-Transform infrared spectrometer (FT-IR) was used to detect the functional groups involved in the bio-production AgNPs through using FT-IR spectrometer (Agilent Cory 630, Agilent Technologies, TX, USA) through an investigation region of 4000-500 cm^{-1}. The particle size of the biosynthesized AgNPs was characterized by dynamic Light Scattering techniques using Zetasizer Nano ZS (Malvern Panalytical, Spectris plc, Egham, Surrey, United Kingdom)

Preparation of AgNPs for Analysis

The Cyanobacteria-AgNPs mixture was centrifuged (12,000 × g, 20 min, 10°C), the supernatant was discarded, and the generated pellets

were rinsed with 10 mL distilled water several times. The pellets were dried (30°C) for 24 hours and then spread in distilled water at the required concentrations.

Antibacterial Bioassay

The antibacterial potency of the produced Ag-NPs was assessed against Methicillin-resistant staphylococcus aureus (MRSA) strain as stated by Hamida et al[12]. They used the Kirby Bauer Disk Diffusion Susceptibility method[13] with some modification. Sterilized-Whatman number 1 paper discs (6 mm in diameter) were saturated with 20 µl of AgNPs solution of the following concentrations (1, 5, 7, 10, 15, 20, and 30 µg/mL). The paper discs were dried and placed on the surface of the inoculated nutrient agar medium with bacterial suspensions prepared in physiological saline. Plates were kept for 2 hrs at 4°C to ensure the diffusion of the bioactive material, after which the plates were incubated at 37°C. Discs containing 20 µl of sterilized distilled water were used as a negative control, whereas the positive control discs contained 0.5% Chloramphenicol. A mixture of the Ag-NPs and Chloramphenicol was used where the required concentration of AgNPs was prepared in 0.5% solution of chloramphenicol and then Sterilized- Whatman number 1 paper discs were impregnated in 20 µl of such solution. The prepared paper discs are lifted to dry and then treated similarly as above. All plates were incubated for 24 h, and the diameters of inhibition zones were measured in triplicates (mm) to be used as an indicator for activity.

In Vivo Wound Healing Assay – Animals

Male Wister Rats (weight 200-300 g) were supplied by the animal house facility, King Saud University, Riyadh (Kingdom of Saudi Arabia). Animals were housed separately in polypropylene cages and maintained under standard housing conditions (room temperature 25 ± 2°C, humidity 50 ± 5°C with 12:12 light: dark cycles), with the exceptional caution for conserving the aseptic condition through the study[14].

Ethical Statement

All experiments were appropriately performed in accordance with the "Ethical Conduct for the Use of Animals in Research" Guidelines in King Faisal University and the "Executive Regulations for Research Ethics on Living Creatures (Second Edition)", published by the National Bioethics Committee, Saudi Arabia. All animal care and experimental procedures were approved by the Animal Research Ethics Committee at King Faisal University.

Experimental Design

Three wound models (excision, incision, and burn) were used to assess the wound healing activity in this study. Rats were randomly divided into five groups in each model (n=8). Group I, was treated with vehicle ointment containing only the bacterial biomass, prepared as mentioned in the section "Preparation of Ag-NPs for analysis" (negative control), Group II, was treated with the commercial standard ointment (Silver Sulfadiazine 1% ointment (SSD) (Dermazin®), manufactured by Medical Union Pharmaceuticals, Saudi Arabia) for wound healing (Positive control), Group III, IV and V treated were treated with 10, 30 and 50 µgAg-NPs/kg ointments, respectively (AgNPs (10 µg/kg); AgNPs (30 µg/kg); AgNPs (50 µg/kg)). Different topical formulations (ointments) were prepared as mentioned elsewhere[4]. Prepared topical preparations were applied once daily, directly on the open wound until the wound was completely healed. No antibiotic was administered to any of the animals' groups, and the animals were monitored daily or any wound contamination.

After complete wound healing, the animals were sacrificed using pentobarbitone sodium (60 mg/kg; i.p.), and tissue specimens were harvested and cut apart along a uniform direction and maintained in liquid nitrogen and physiological saline solution for biochemical and tensile strength analysis.

Excision Wound Model

The model was adopted from Naraginti et al[4] with minor modifications. In brief, the animals were anesthetized (mild ether), the excision wound outline (approximately 500 mm^2 circular area) was marked on the shaved dorsal portion, and then, a wound (2 mm thickness) was created at the marked area using a sterilized sharp surgical blade. The wound was cleaned with a sterile cotton wipe dipped in normal saline and then treated with their above-mentioned respective group topical treatments. Wounds were kept without dressing throughout the experimental duration. Topical treatment continued until complete full epithelization was achieved, and the number of days taken

to reach full epithelization point was recorded, considering the day of wound creation as day 0. Photographs were taken for each wound with a digital camera.

Incision Wound Model

This model was implemented according to Pannerselvam et al[5]. Briefly, 8 cm straightforward incision was performed paravertebrally through the whole thickness of the skin, on either side of the vertebral column, with a sharp, sterile scalpel, then an interrupted suture (about 1 cm apart) was used to close the wound. Days of topical preparations' application started from day 0 to day until day 21 post-wounding.

Burn Injury Model

This model was implemented according to Zhang et al[6]. Overnight fasted animals were anesthetized using ether, and their back was shaved to induce burn wound. Hot molten wax (70ºC) was poured onto the shaven back from cylinder has 400 mm^2 circular openings and remained on the skin until solidified. The wax was removed with caution, and the above prepared topical formulation was applied once daily until epithelization was complete. Treatment continued, and the endpoint of epithelization was taken as the sloughing of the scar, leaving no raw wound behind.

Wound Area Parameters

Wound area: the progressive changes in the open wound area edges were measured by tracing the outline of the wound onto millimeter-scale graph paper, and the percentage of wound healing was calculated as the change in the original wound size for each animal on predetermined days post-wounding.

Epithelialization time: it is the number of days taken to drop off the dead tissue without any sign of raw wound, and it was measured from day 0 as formerly stated[3,15].

Wound contraction percentage: it was calculated as mentioned earlier[4,16] using the below equation: wound contraction percentage = ((wound area day 0-wound area day X)/wound area day 0) × 100 where X represents the number of days until complete healing.

Skin Tissues Measured Parameters

Hydroxyproline content: the hydroxyproline content in wound tissues was determined as described earlier[16]. Briefly, the wound tissues were dried in a hot air oven at 60°C to a constant weight and then hydrolyzed with 6 N Hydrochloric acid (HCl) (1:10, w:v) at 130°C for 4 h in sealed glass tubes. The hydrolysates were neutralized to pH 7.0 and then subjected to oxidation *via* Chloramine T. The reactions were terminated by the addition of perchloric acid (0.4 M), and the colors were then developed using Ehrlich reagent at 60°C and measured at 557 nm. The hydroxyproline concentrations were calculated from the standard linear curve and presented as mg/g of dry tissue weight.

Antioxidant enzymes: the supernatants from wound tissues homogenates were used to evaluate the activity of the numerous antioxidant enzymes, including catalase (CAT, Cat. No.707002), superoxide dismutase (SOD, Cat. No. 706002), and Glutathione peroxidase (GPx) using corresponding ELISA kits (all obtained from Cayman Chemicals (Ann Arbor, MI, USA) and according to the manufacturer protocols.

Lipid peroxidation assay: the lipid peroxidation in supernatants from wound tissue homogenates was determined by thiobarbituric acid reaction and expressed as malondialdehyde (MDA) level using thiobarbituric acid-reactive substances (TBARS) assay as stated elsewhere[16]. TBARS kit (Cat. No. ab 118790) was obtained from Abcam (Cambridge, MA, USA). The absorbance was determined at 530 nm, and the results were expressed as the amount of MDA (nmol) per mg of protein.

Cytokines determination: expression patterns of interleukin-6 (IL-6, Cat. No. ab100772), interleukin-10 (IL-10, Cat. No. ab100764), and IFN-γ (Cat. No. ab239425) were investigated in different days of the experiment by ELISA kits using the supernatants from serum obtained from Abcam (Cambridge, MA, USA).

Estimation of tensile strength implemented according to Pannerselvam et al[5] and Yadav et al[15]. This parameter was measured in cases of incision and burn wounds models. Skin area was incised 1.5 cm (in incision wounds, after 21 days) and 1 cm (in burn wounds, after 18 days) away from each side of the wound, align with the anterior-posterior axis of the animal to warrant samples consistency. Additionally, the thickness of the skin and the width of the gauge regions were measured with Vernier calipers before loading. The obtained wound tissues were used to measure the load (force) required to break the tissue with a computerized tensiometer (EZTESTI 30804100798, Shimadzu Corp., Japan). Tensile strength was calculated using the following for-

mula: Tensile strength (N/cm^2) = Breaking force (N)/ Area cm^2 where area (cm^2) = thickness (cm) × width (cm).

Results

The biosynthesis of nanosilver was indicated by the change in the reaction mixture, containing the cyanobacterial cell and $AgNO_3$, in relation to the negative control, which verified the production of AgNPs by the organism. The transit color change from yellowish green to brown implies the reduction of Ag^+ ion to Ag^0 and the formation of AgNPs. Dynamic light scattering technique was used to measure the particle size of the produced AgNPs to be 86.38 (± 3.364) nm (Figure 1A).

UV-Visible Spectrometric Profile of AgNPs Produced by Phormidium sp.

Figure 1B illustrated the presence of AgNPs surface plasmon resonance (SPR) peak at 440 nm after the addition of 0.5 mM $AgNO_3$ to the cyanobacterial cells, and the intensity increased with time until reaching the maximum after 48 hours. This is in accordance with the characteristic bands in the UV-Visible spectrometric analysis indicative of silver nanoparticles, which showed plasmon resonance in the range of 410-450 nm[17].

FT-IR Spectrometric Profile of AgNPs Produced by Phormidium sp.

FT-IR can aid in revealing the potential secondary metabolites or at least the functional groups that may contribute to the reduction of the silver ion and formation of the nanoparticles or those involved in the stabilization of the nanoparticles produced. Figure 1C illustrates the FT-IR profile, which indicates the presence of 20 peaks for the Phormidium sp. extract directly after the addition of $AgNO_3$ (zero time), whereas the same mixture after 48 hours showed 14 bands (Figure 1D). Figure 1 C and D showed distinctive broadband at around 3100-3500 cm^{-1} representing the hydroxyl group stretching vibration, indicating the presence of hydroxyl functional groups type. The peak shifting in AgNPs spectral profile (Figure 1D) could be attributed to the interactions between functional groups responsible for those bands and AgNPs[18]. In the hereby study, the shifting for the broad hydroxyl band from 3417 to 3441 cm^{-1} could be explained by the interaction of hydroxyl groups of polyphenols or sugars in the cyanobacterial extract with the produced AgNPs. The presence

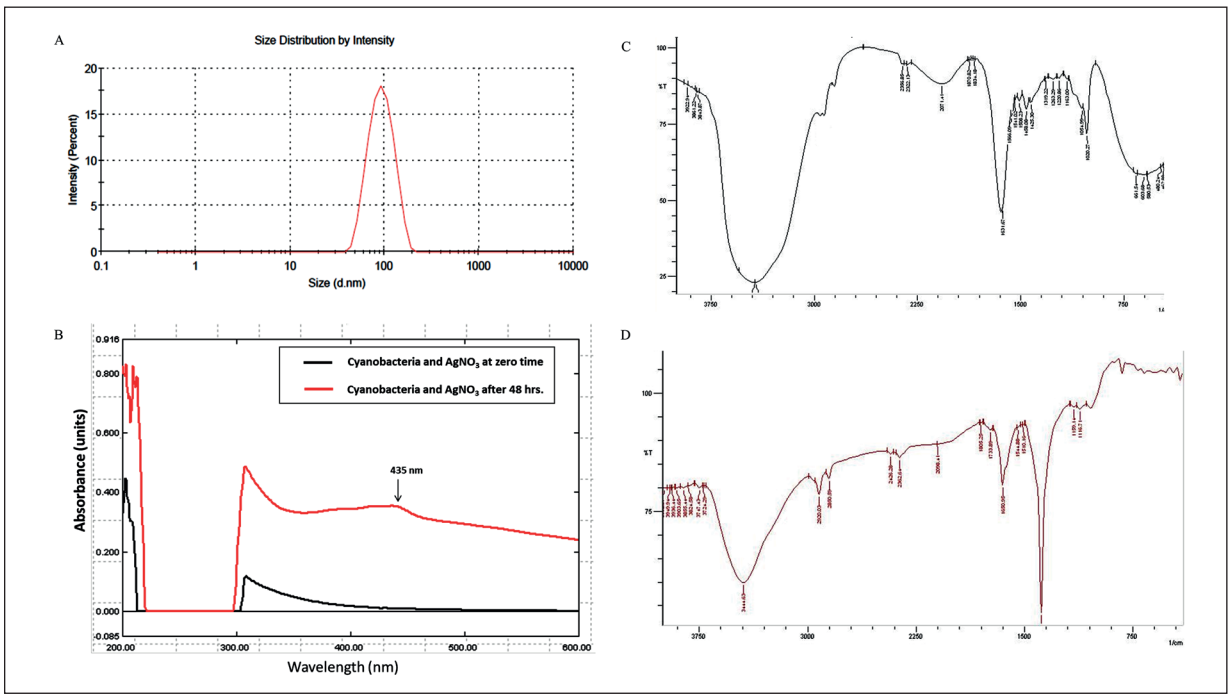

Figure 1. Characterization of biogenic AgNPs synthesized by *Phormidium* sp. **A,** Dynamic scattering graph identifying the particle size. **B,** UV–Vis light spectrometry. **C,** FTIR spectrum of Cyanobacterial extract at zero time directly after addition of $AgNO_3$. **D,** FTIR spectrum of Cyanobacterial extract after 48 hours of $AgNO_3$ addition.

of a unique peak of 2920 cm^{-1} represents the C-H stretching vibration could indicate the involvement of hydrocarbon chains in the stabilization of Ag-NPs. The involvement of amide groups (might be from amino acids, peptides or proteins) could be suggested from the band at 1650 cm^{-1}, shifted from 1631 cm^{-1}, assigned to the stretching vibration of (NH) C=O group (Amide band II) and the band 1382 cm^{-1} (shifted from 1319 cm^{-1}) and assigned for C–C and C–N stretching vibrations[19]. The carboxyl and N-H groups of amides are used to stabilize the formed AgNPs through surrounding the nanoparticle by proteins[20].

Antibacterial Assay of Phormidium sp.-AgNPs

AgNPs produced by *Phormidium* sp. were evaluated for their anti-MRSA activity using the disc diffusion method. Several concentrations of the cyanobacterial-AgNPs extracts were investigated, and the lowest concentration with significant action was 5 µg/ml; however, the optimum concentration was 20 µg/ml, which was able to produce 1.3-fold activity more than the positive control (0.5% chloramphenicol) (Figure 2A). When the same concentration (20 µg/ml) of *Phormidium* sp.-AgNPs

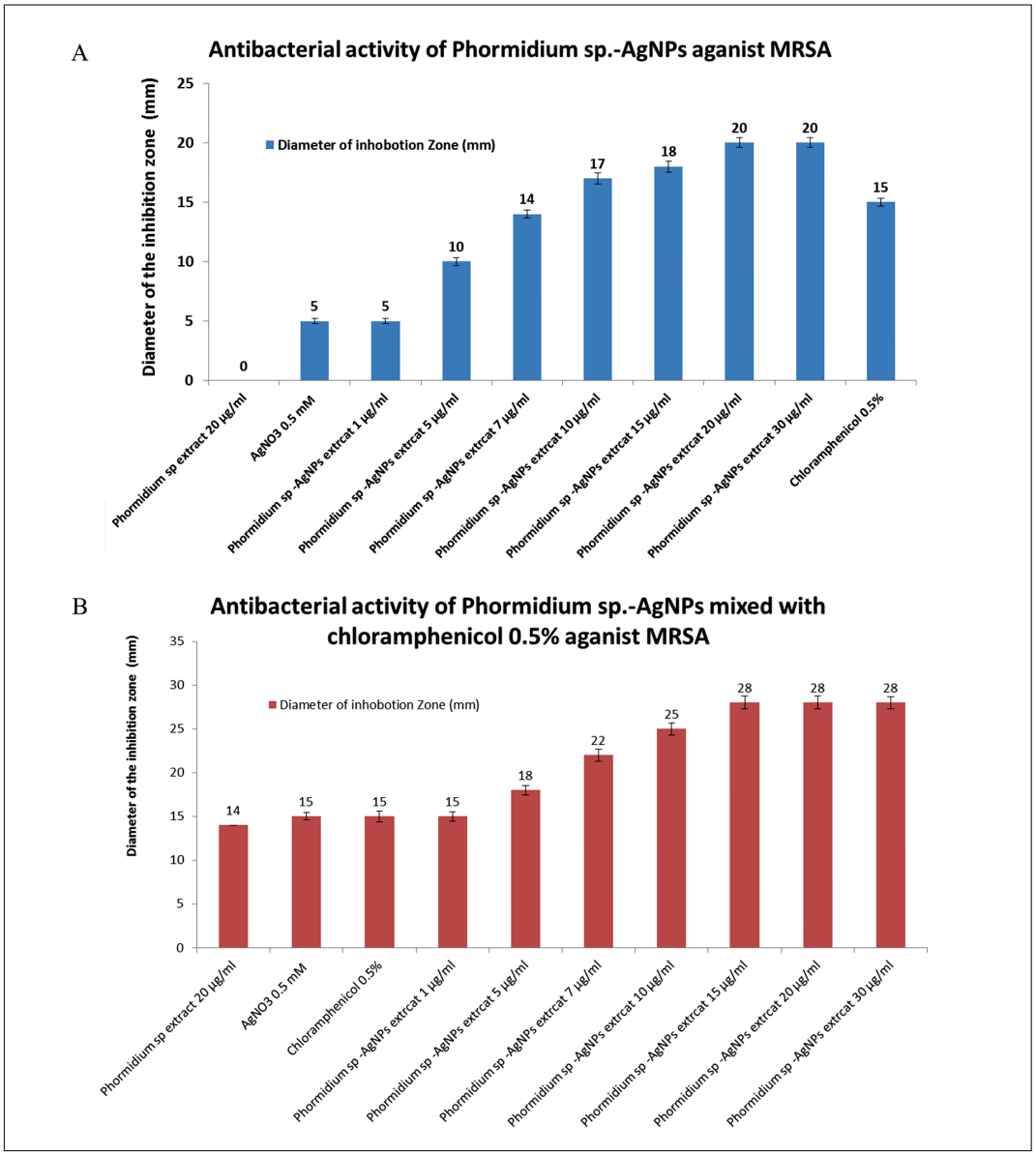

Figure 2. Disc inhibition zone against MRSA. **A,** *Phormidium* sp.-AgNPs. **B,** a mixture of *Phormidium* sp.-AgNPs and 0.5% chloramphenicol.

extract was combined with 0.5% chloramphenicol, the antibacterial activity increased nearly to double (1.86 fold) than the 0.5% chloramphenicol alone (Figure 2B).

Wound Healing Assay

The effect of AgNPs produced by the *cyanobacterium Phormidium* sp. on different types of wounds was scrutinized hereby. Neither abnormal clinical signs nor mortality was observed on the general health or behavior of the animals during the whole period of the study. AgNPs-treated wounds exhibited no evidence of microbial contamination, bleeding or pus formation during treatment, whereas control wounds revealed notable inflammation. We observed an insignificant increase in the weights of rats of different groups after each treatment, suggesting a normal animal growth cycle during the whole study. All models showed very similar results related to skin tissue parameters and cytokines evolution, so we only represented the results related to the excision model. The tensile strength estimation experiment was applied in the incision and burn wound models.

Excision Wound Healing Evaluation – Wound Area Contraction and Epithelialization

We utilized the changes in wound color and inflammation status, and wound area reduction as parameters to appraise the wound healing process. Representative wound photographs from each investigational group were taken on different days to estimate the potential of AgNPs on the wound healing process (Figure 3). On the first day of wound injury, a bright red color was observed in all wounds, indicating that the blood was recovered to the underlying muscle after the skin injury. After three days of healing, a growing fresh skin after AgNPs treatments appeared smoother and leaves less scab than those of control groups reflecting the wound healing process initiation. After seven days, a dark brown color was detected for the treated groups signifying the scab formation, while the untreated negative wounds were still faintly red and swollen. On the 14th day, AgNPs treated wounds were significantly reduced in size with 81.39%, 89.39%, and 90.45%, respectively, as compared to untreated negative control and positive control groups (55.32% and 73.39%, respectively) (Figure 3, Table I). As compared to the

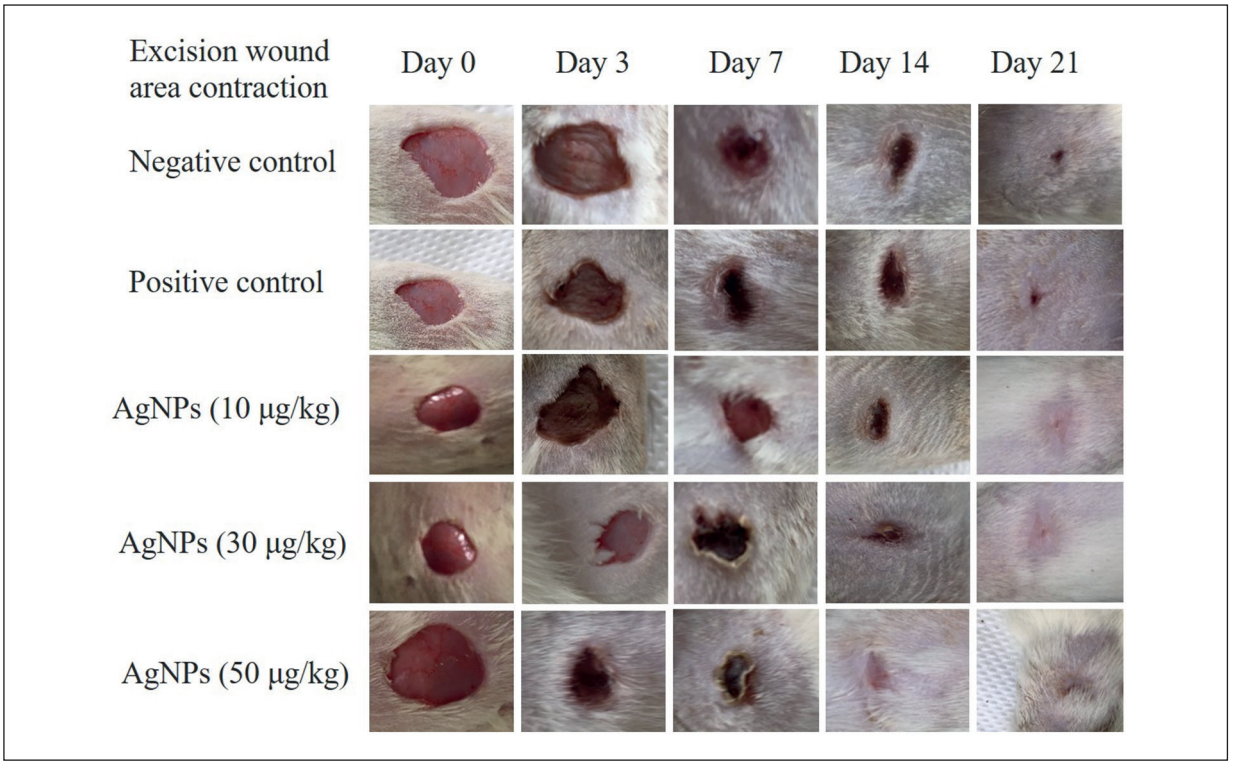

Figure 3. Photographic representation of wound healing process in excision wound model from different experimental groups at 0, 3, 7, 14, and 21 days of post wounding.

Table I. Percentage of wound contraction using the excision wound in the different experimental groups.

Groups	Epithelization period (days)	Percentage of wound contraction			
		3rd day	7th day	14th day	21st day
Negative control	23.5 ± 1.12	20.43 ± 0.89	40.32 ± 0.55	55.32 ± 2.51	85.87 ± 0.65
Positive control	19.0 ± 2.1	27.98 ± 1.08	46.21 ± 0.87	80.39 ± 1.45	100
AgNPs (10 µg/kg)	17.5 ± 2.5	25.95 ± 0.81	55.83 ± 2.32	81.39 ± 3.74	98.45 ± 5.43
AgNPs (30 µg/kg)	16.0 ± 2.0	25.67 ± 1.35	57.83 ± 1.53	85.39 ± 4.77	100
AgNPs (50 µg/kg)	15.0 ± 1.5	26.67 ± 1.02	62.05 ± 2.92	86.45 ± 3.65	100

control groups, the scab formation substantially reduced, and the wound area was significantly decreased in AgNPs treated groups ($p < 0.05$). After 21 days of wound injury, the untreated rats still show an open wound (about 15%), in contrast to the treated groups in which a total contraction of wounds (almost 100%) was achieved. The wound contraction percentage results in days 7, 14, and 21 showed significant differences between all the tested groups with the maximum seen in AgNPs (50 µg/kg) after day 7 (Table I). The mean period of epithelialization decreased from 23.5 ± 1.12 days in the negative control group to 17.5 ± 2.5 in AgNPs (100 µg/kg) group with no significant differences between different concentrations of AgNPs groups (Table I).

Evaluation of Skin Tissues Measured Parameters

Collagen is the principal extracellular protein in the skin tissue, and hydroxyproline is the main element of collagen, which makes it an excellent biochemical marker for collagen content within the tissue. Therefore, hydroxyproline level is frequently used as a positive marker of wound healing[15,16], since hydroxyproline amount intensification can indicate any alteration of collagen synthesis and reflects the process of wound healing in the damaged tissues. Figure 4 indicated a significant increase in hydroxyproline levels for AgNPs treated groups (22.16, 26.15, and 33.01 mg/g of tissue), respectively, when compared to the negative untreated control (17.37 mg/g of tissue) and positive treated groups (32.78 mg/g of tissue), indicating that AgNPs induced collagen production.

Furthermore, Figure 4 showed a notable reduction in MDA level (as a marker for lipid peroxidation) in the tissue obtained from animals treated with AgNPs in a dose-dependent manner (1.27, 1.14 and 0.86 nmole MDA/mg of protein, respectively) as compared to positive

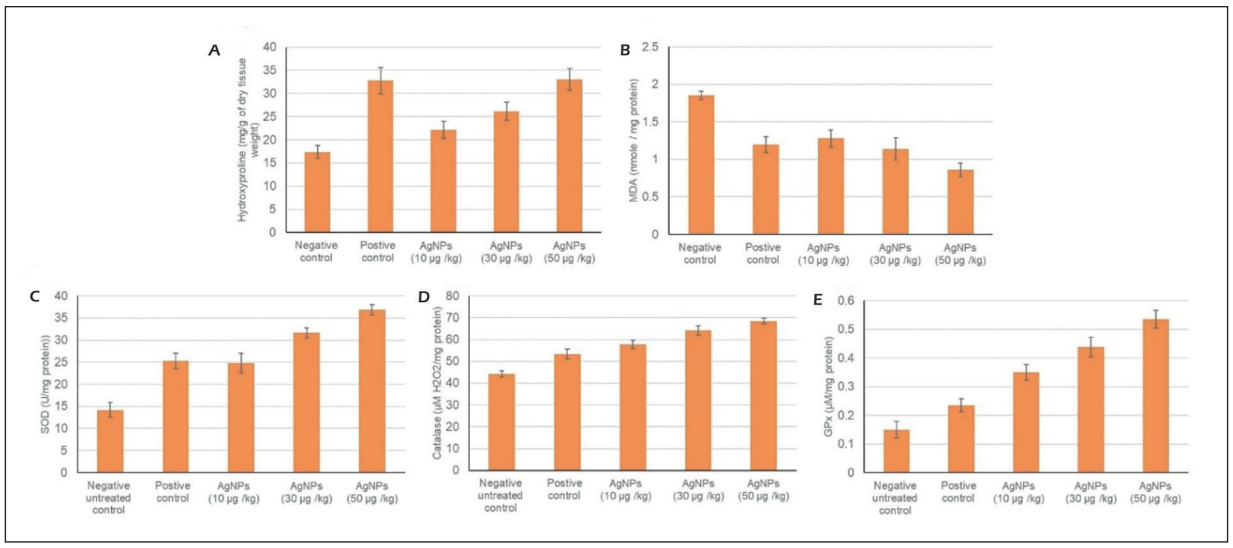

Figure 4. Effect of biogenic AgNPs synthesized by *Phormidium* sp. on **(A)** hydroxyproline content; **(B)** MDA (Lipid peroxidation product); **(C)** Superoxide dismutase (SOD); **(D)** Catalase, and **(E)** GPx (antioxidant enzymes) in excision wound model.

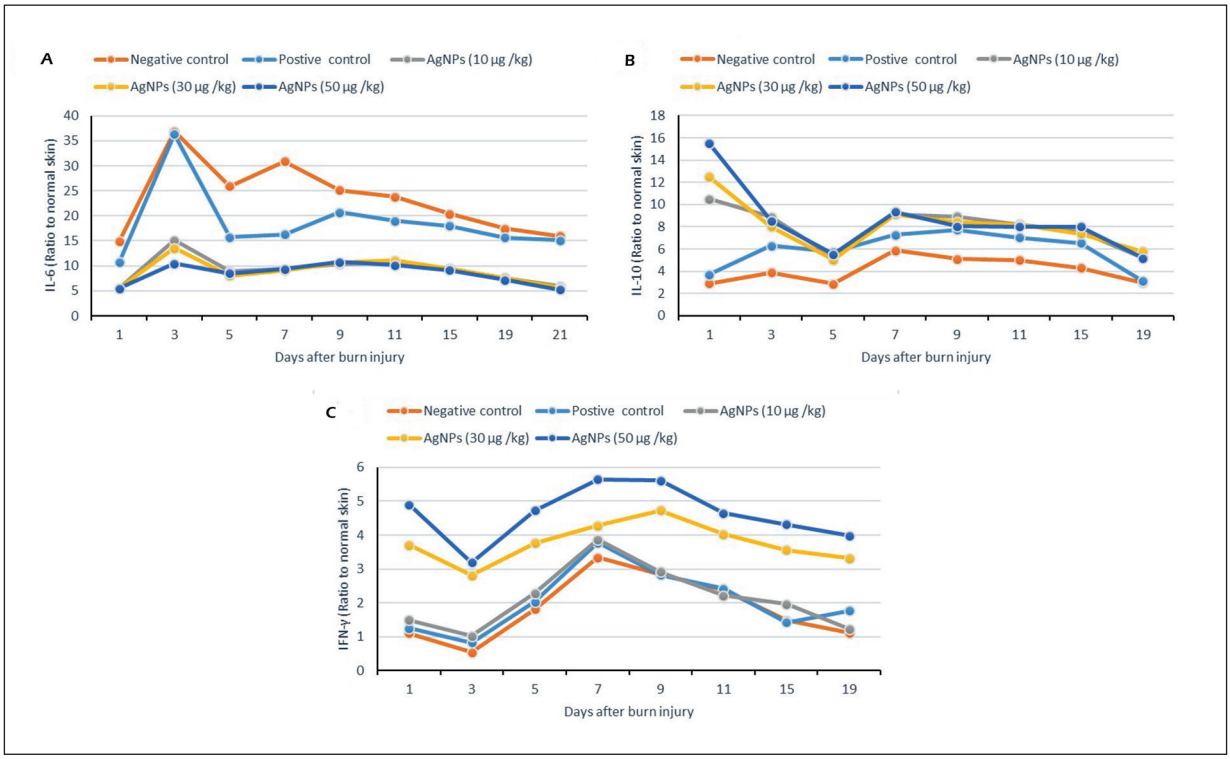

Figure 5. Modulation of cytokine profile by AgNPs synthesized by *Phormidium* sp.. (**A**) IL-6; (**B**) IL-10 and (**C**) IFN-γ at various time intervals after excision injury.

control group tissue (1.19 nmole MDA/mg of protein), and the negative control group tissue (1.85 nmole MDA/mg of protein). Results indicated that the use of AgNPs significantly reduced the secondary oxidation product content (MDA).

Figure 4 presented a significant elevation in antioxidant enzymes (CAT, SOD, and GPx) amounts in the wound tissue homogenates treated with AgNPs, as compared to untreated groups. This elevation could be attributed to the decrease in reactive oxygen species (ROS) production. For example, GPx activity raised up from 0.15 µM/mg protein (negative control) to 0.35, 0.43, and 0.53 µM/mg of protein in AgNPs groups, respectively signifying that AgNPs exposures increased the peroxidase activity.

Evaluation of Cytokines

Figure 5 described the levels of IL-6, IL-10, and IFN-γ (cytokines) in the wounded animals' blood during the whole period of the study. AgNPs topical treatment kept IL-6 significantly lower throughout the healing process even when compared with the positive control group, while stimulated the production of cytokines IL-10 and IFN-γ, which enhance scarless wound healing processes. The differences attained in the levels of various cytokines show that AgNPs can modulate cytokine expression in a dose-dependent manner.

Incision Wound Healing Evaluation – Tensile Strength Estimation in an Incision Wound Model

On the 15th day, tensile strength for each group was measured and reported in Table II. Breaking strength was found to be highest in the 50 µg AgNPs/kg followed by 10 µg AgNPs/kg and 30 µg AgNPs/kg groups and finally positive control as compared to the negative control group.

Table II. Tensile strength using the incision wound model in the different experimental groups.

Groups	Tensile strength (N/cm^2)
Negative control	16.39 ± 2.7
Positive control	23.54 ± 2.44
AgNPs (10 µg/kg)	25.43 ± 5.4
AgNPs (30 µg/kg)	26.87 ± 3.9
AgNPs (50 µg/kg)	30.65 ± 4.2

Burn wound healing evaluation – Wound Area Contraction and Epithelialization

Topical application of positive control and AgNPs considerably reduced the epithelization period as well as an upsurge in wound contraction ($p < 0.05$), when compared to the negative control (Figure 6, Table III).

On day 1, the burn wounds in all experimental animals were swollen and bruised. On the 6th day, the animals treated with AgNPs and positive control showed dark reddening and thickening of the wounded skin, whereas the wounds of the untreated group of animals did not show any thickening of the skin. On the 6th day, the topical preparation with AgNPs (50 µg/kg) showed a 26.01% wound contraction, which could be compared with the positive control (25.81%) on the same day with no significant difference between both groups. This healing effect of AgNPs continues till the 18th day with 85.81% wound contraction for the same AgNPs groups, which again could be compared to the positive control (Figure 6, Table III). The burn wounds treated either with different concentrations of AgNPs or with positive control preparations showed higher wound contraction percentages relative to the negative control. On the 12th day, the wounds treated either with different concentrations of AgNPs or positive control preparations showed moderate exudation and hair growth, with scabs covering the wound surface. By contrast, the negative control group did not show any hair growth or scab covering. Furthermore, the burn wounds of the AgNPs treated groups displayed a dry surface, progressive wound contraction, and increased hair growth. On the 18th day, the wounds treated with different concentrations of AgNPs showed a marked reduction in size and hair growth around the wound site.

The mean period of epithelialization decreased from 20.0 ± 1.2 days in the negative control group to 15.46 ± 2.7 in AgNPs (30 µg/kg) group with no significant differences between the 30 µg/kg and 50 µg/kg AgNPs groups (Table III).

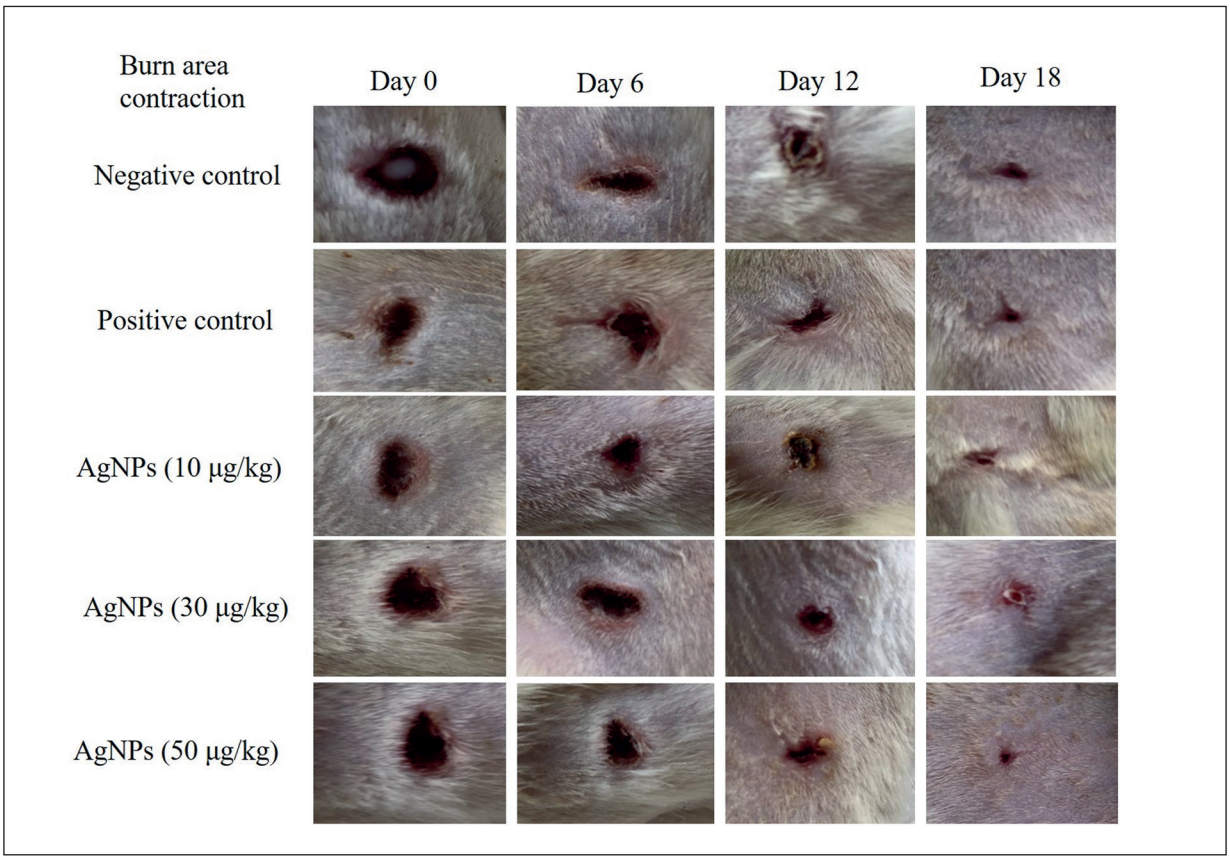

Figure 6. Photographic representation of wound healing in burn wound model from different experimental groups at 0, 6, 12, and 18 days of post wounding.

Table III. The effect of AgNPs on the burn wound contraction of experimental rats.

Groups	Epithelization period (days)	Percentage of wound contraction		
		6th day	12nd day	18th day
Negative control	20.0 ± 1.2	10.25	27.50	29.57
Positive control	15.0 ± 2.1	25.81	64.52	83.89
AgNPs (10 µg/kg)	17.0 ± 1.5	14.90	36.13	62.16
AgNPs (30 µg/kg)	15.46 ± 2.7	18.75	53.12	76.12
AgNPs (50 µg/kg)	14.5 ± 1.5	26.01	58.71	85.81

Estimation of Tensile Strength

Application of AgNPs with different concentration to animals' burns significantly increased the average yielding load of the skin to 19.82 ± 3.11, 25.74 ± 3.24, and 34.83 ± 2.24 for AgNPs (10, 30, and 50 µg/kg), respectively (Table IV), relative to the negative and positive controls (13.15 ± 1.71 and 30.22 ± 3.14, respectively). The tensile strength increased with AgNPs preparation application in a concentration-dependent manner until the AgNPs (50 µg/kg) could be compared with the positive control, showing no significant difference between both groups.

Discussion

Green synthesis of metal nanoparticles is priv ileged over both the chemical and physical methods being eco-friendly, cost-effective, easily be scaled up for mass production, and the lack of toxic chemicals usage. Cyanobacteria have proved in many instances their potential to produce several metal nanoparticles, including Nobel metals such as gold and silver, as a method for environmental detoxification. Some common cyanobacterial genera that were proven to possess such capability are Anabaena, Calothrix, and Leptolyngbya[21]. In the hereby study, we tried to prove the ability of cyanobacteria from the genus *Phormidium* to produce AgNPs, together with the ability of the cyanobacteria-AgNPs to heal wounds in experimental animals.

Table IV. The effect of AgNPs on the tensile strength and epithelization period of burn model experimental rats.

Groups	Tensile strength (N/cm²)
Negative control	13.15 ± 1.71
Positive control	30.22 ± 3.14
AgNPs (10 µg/kg)	19.82 ± 3.11
AgNPs (30 µg/kg)	25.74 ± 3.24

Antibacterial Action

The control of infections represents a critical aspect in wounds management. In damaged skin, bacteria can reach the underlying tissues causing inflammation, which leads to the release of proteases and reactive oxygen species from inflammatory cells[2]. Numerous studies[3,4] described the topical application of silver for antimicrobial and wound healing applications. Silver ions inhibit bacterial enzymes by binding to DNA, whereas AgNPs prompt bacterial cell wall as well as cytoplasmic membrane damage[4].

Methicillin-resistant *Staphylococcus aureus* (MRSA) is a bacterium that infects different parts of the body; however, like other staphylococcus strains, it is most likely to cause skin infections. MRSA is resistant to many antibiotics; therefore, many approaches were investigated to decrease bacterial resistance, and one of these approaches is to use a combination of the antibiotic with other bactericidal or bacteriostatic agents. The study hereby tried to use the cyanobacterial generated silver nanoparticles alone and in combination with 0.5% chloramphenicol to inhibit the growth of MRSA. The presence of silver nanoparticles augmented and reinforced the effect of Chloramphenicol against MRSA. Similar effects were reported before; for example, Surwade et al[22] reported the potentiation of the ampicillin effect on MRSA in the presence of 25 µg/ml AgNPs. Similarly, Abdel Rahim and Ali Mohamed[23] reported an increase in ampicillin activity as the concentration of combined AgNPs increased. The types of studies, such as the hereby study, can add more to the growing pool of the term Nanoparticle-based antibiotic constructs or Nanoantibiotics has become now more and more popular[24].

Wound Healing Properties

The results of the present study revealed epithelialization, tensile, and hydroxyproline content amplification in animals treated with AgNPs due

to the strengthening effect and maturation of collagen fibers synthesized in granulation tissue. Likewise, Tian et al[25] reported that AgNPs applied topically in animal burn models reduced wound inflammation and modulated the fibrogenic cytokines, contributing to wound healing. Also, Wasef et al[26] showed that AgNPs-treated skin exhibited less epidermal necrosis and losses, lower collagen degeneration, and granulation tissue formation, epidermal regeneration.

Tensile strength is a major index of wound repairing and strength since it indicates the subdermal formation and deposition of the newly formed collagen fibers[15]. At the beginning of the healing process, a wound has little breaking strength, but as it heals, the breaking strength increases rapidly due to the synthesis of collagen and the formation of stable intraand intermolecular crosslinking[3]. Wound curative agent should accelerate the viability of collagen fibers to increases wound tensile strength[15]. A main element of collagen is hydroxyproline, which makes it an excellent biochemical marker for collagen content within the tissue[15,16]. Therefore, hydroxyproline amount intensification can be used as an indication of collagen synthesis rates, and any alteration of collagen synthesis reflects the process of wound healing in the damaged tissues[25].

Lipid peroxidation of unsaturated lipids produces a wide variety of secondary oxidation products; amongst is malondialdehyde (MDA), which has extensively been benefited from as an appropriate biomarker for lipid peroxidation of polyunsaturated fatty acids[16,25]. Notable reduction in the MDA level was observed in the tissue obtained from animals treated with AgNPs as compared to control group tissue indicating that AgNPs significantly reduced the secondary lipid peroxidation products content, which is in harmony with results previously described by Tian et al[25]. Free radical and oxidative reaction products generate tissue damage and are particularly encountered during connective tissue disorders like fibrosis during wound healing[16]. Free radical formation, together with the lack of ability to scavenge reactive oxygen species, are causative factors of various skin lesions, and it interferes in the proliferation of fibroblast. Tissue wound responds to an increase in oxidative stress followed by the damaging effect on the cellular membrane, DNA, proteins, and lipid molecules results in the delay in the healing process[15,16]. Acceleration of the healing process could be achieved by the removal of these reactive oxygen species. Hence, granulation tissue estimation for antioxidant enzyme activity is pertinent to pace up the repairing of wound tissue[15]. The results of the present study showed that AgNPs treatment significantly elevated the level of antioxidant enzymes, i.e., SOD, CAT, and GPx. Tian et al[25] showed that the silver nanoparticles were able to avoid antibacterial contamination, reduce wound inflammation, modulate fibrogenic cytokines, and contribute the wound healing acceleration.

Multiple growth factors and cytokines released at the wound site strictly regulate wound healing and, due to the complex nature of the process, many factors can interfere in delaying wound healing, increasing patient morbidity, and mortality, and resulting in a low cosmetic outcome and significant discomfort and distress[2]. As a result, the inflammation process acts as a crucial part of wound healing to avert the growth of pathogens in the wound area, which leads to shun an infection and ultimately increases the number of fibroblast cells along with the formation of collagen[15]. Although cytokines are crucial in initiating, sustaining, and regulating the post-injury response, these same molecules have been implicated in impaired wound healing, abnormal scar formation, and uncontrolled inflammatory response[25]. Keratinocytes at the skin wound secrete several pro-inflammatory mediators, including IL-1α, IL-6, IL-8, IL-15, IL-20, TNF-α, CXCL10, and CCL20 (MIP-3α), and play an important role in the recruitment and activation of neutrophils[6]. Lack of amplification of the inflammatory cytokine cascade may be important in providing a permissive environment for scarless wound repair to proceed[25]. One of the unique actions of IL-10 is its ability to inhibit the synthesis of pro-inflammatory cytokines, including IL-6, leading to matrix deposition reduction and scar-free healing[25]. IL-6 is an important cytokine involved in the early inflammation of burn injury, with its level peaking on post-burn days 3-4[6]. IL-6 further enhances the effect of TNF-α and IL-1, which combine to amplify the inflammatory response in the post-burn period[6]. Decreased IL-6 resulted in fewer neutrophils and macrophages recruited to the wound and fewer cytokines being released in the wound with subsequently lower paracrine stimulation of cellular proliferation, fibroblast and keratinocyte migration, and extracellular matrix production[25]. Interferon-γ (IFN-γ) production by T lymphocytes and macrophages plays an important role in the tissue remodeling of wounds[25]. The reduc-

tion of wound contraction by IFN-γ is mediated by retarding collagen production and lattice cross-linking with an increase in collagenase production[25]. As IFN-γ has been demonstrated as a potent antagonist of fibrogenesis through its ability to inhibit fibroblast proliferation and matrix production, its control on TGF-β production may play a role[25]. In the current study, AgNPs suppressed the production of IL-6, pro-inflammatory cytokines, but stimulated the production of an anti-inflammatory cytokine IL-10 and IFN-γ. Earlier reports similarly proved that AgNPs suppressed the production of the pro-inflammatory cytokines, such as IL-6 mRNA, but promote the production of an anti-inflammatory cytokine IL-10, VEGF, and IFN-γ mRNA at the skin wound, indicating that AgNPs suppress inflammation[6]. AgNPs regulated pro-inflammatory cytokine IL-6 production of keratinocytes and neutrophils infiltration through KGF-2/p38 signaling pathway[6]. Wasef et al[26] demonstrated that AgNPs upregulate the expression of interleukin-1 (IL-1) and interleukin-6 (IL-6) in macrophage cells. Furthermore, several reports have documented that suppressing inflammation by silver nanoparticles promoted wound healing in burn injury mouse models[5,6,26], in full-thickness incision mouse model[5], and in contact dermatitis porcine model.

Conclusions

In summary, AgNPs are produced from the *cyanobacteria Phormidium* sp. AgNPs are characterized using UV and FTIR spectrophotometry. The antibacterial of the produced AgNPs against MRSA was proven, and the nanoparticles showed a potentiation effect for the bactericidal effect of the antibiotic chloramphenicol against the same bacteria. The green synthesized AgNPs have demonstrated effectiveness in the wound healing process in rat models. The results provided a scientific validation of wound healing potency of AgNPs (10, 30, and 50 μg/kg) in different wound models (excision, incision, and burn) when topically applied. Wound healing potency was confirmed by the significant improvement and increase in the rate of wound closure, hydroxyproline content, and the reduction in epithelialization period of granulation tissue. The substantial effect of wound repairing was further supported by enzymatic antioxidant level escalation and inflammatory cytokines attenuation. Our findings indicate the efficient antioxidant property of silver nanoparticles and implicate the ability of silver to modulate the cytokines involved in wound healing. Biogenic AgNPs produced by *Phormidium* sp. showed significant antimicrobial together with wound healing abilities.

Conflict of Interest

The Authors declare that they have no conflict of interests.

Acknowledgements

The authors are grateful to the Dean of Scientific Research at King Faisal University for financial support.

Funding

This research was funded by Deanship of Scientific Research, King Faisal University, Kingdom of Saudi Arabia grant number [17122009]. The authors express their deepest gratitude for the Deanship of Scientific Research for financial and moral support.

Authors' Contribution

Conceptualization was done by all authors, N.S.Y., M.E.M., N.A.E.S.; methodology, N.S.Y., N.A.E.S.; validation, N.S.Y., and N.A.E.S.; formal analysis, N.S.Y.; resources, N.S.Y., and N.A.E.S.; data curation, M.E.M., N.S.Y., and N.A.E.S; writing original draft preparation, N.S.Y., M.E.M., N.A.E.S; writing review and editing, M.E.M, N.S.Y., project administration, N.A.E.S..; funding acquisition, N.A.E.S.

Nancy Safwat Younis

orcid.org/0000-0003-4309-7095; Nermin Adel El Semary: orcid.org/0000-0003-3179-0351; Maged E Mohamed: orcid.org/0000-0002-1216-803.

References

1) Sood R, Chopra DS. Optimization of reaction conditions to fabricate Ocimum sanctum synthesized silver nanoparticles and its application to nano-gel systems for burn wounds. Mater Sci Eng C Mater Biol Appl 2018; 92: 575-589.
2) Paladini F, Pollini M. Antimicrobial silver nanoparticles for wound healing application: progress and future trends. Materials (Basel) 2019; 12: 2540.
3) Toppo FA, Pawar RS. Appraisal on the wound healing activity of different extracts obtained from Aegle marmelos and Mucuna pruriens by in vivo experimental models. Niger J Clin Pract 2016; 19: 753-760.
4) Naraginti S, Kumari PL, Das RK, Sivakumar A, Patil SH, Andhalkar VV. Amelioration of excision wounds by topical application of green synthe-

sized, formulated silver and gold nanoparticles in albino Wistar rats. Mater Sci Eng C Mater Biol Appl 2016; 62: 293-300.

5) Pannerselvam B, Dharmalingam Jothinathan MK, Rajenderan M, Perumal P, Pudupalayam Thangavelu K, Kim HJ, Singh V, Rangarajulu SK. An in vitro study on the burn wound healing activity of cotton fabrics incorporated with phytosynthesized silver nanoparticles in male Wistar albino rats. Eur J Pharm Sci 2017; 100: 187-196.
6) Zhang K, Lui VCH, Chen Y, Lok CN, Wong KKY. Delayed application of silver nanoparticles reveals the role of early inflammation in burn wound healing. Sci Rep 2020; 10: 6338.
7) Xu C, van Zalinge H, Pearson JL, Glidle A, Cooper JM, Cumming DR, Haiss W, Yao J, Schiffrin DJ, Proupín-Pérez M, Cosstick R, Nichols RJ. A combined top-down bottom-up approach for introducing nanoparticle networks into nanoelectrode gaps. Nanotechnology 2006; 17: 3333-3339.
8) Makarov VV, Love AJ, Sinitsyna OV, Makarova SS, Yaminsky IV, Taliansky ME, Kalinina NO. "Green" nanotechnologies: synthesis of metal nanoparticles using plants. Acta Naturae 2014; 6: 35-44.
9) Lengke MF, Fleet ME, Southam G. Bioaccumulation of gold by filamentous cyanobacteria Bebween 25 and 200°C. Geomicrobiol J 2006; 23: 591-597.
10) El Semary NA, Mahdi H, Alnoaim A, Alsofan KH, Almsthi SI, Albader WS. Use of algae from an oasis in Saudi Arabia in production of biofuel and bio-fertilizer. Bangladesh Journal of Botany 2018; 47: 523-531.
11) Hamouda RA, Hussein MH, Abo-Elmagd RA, Bawazir SS. Synthesis and biological characterization of silver nanoparticles derived from the cyanobacterium Oscillatoria limnetica. Sci Rep 2019; 9: 13071.
12) Hamida RS, Abdelmeguid NE, Ali MA, Bin-Meferij MM, Khalil MI. Synthesis of silver nanoparticles using a novel cyanobacteria desertifilum sp. extract: their antibacterial and cytotoxicity effects. Int J Nanomedicine 2020; 15: 49-63.
13) Bauer AW, Kirby WM, Sherris JC, Turck M. Antibiotic susceptibility testing by a standardized single disk method. Am J Clin Pathol 1966; 45: 493-496.
14) Pourali P, Yahyaei B. Biological production of silver nanoparticles by soil isolated bacteria and preliminary study of their cytotoxicity and cutaneous wound healing efficiency in rat. J Trace Elem Med Biol 2016; 34: 22-31.
15) Yadav E, Singh D, Yadav P, Verma A. Attenuation of dermal wounds via downregulating oxidative stress and inflammatory markers by protocatechuic acid rich n-butanol fraction of Trianthema portulacastrum Linn. in wistar albino rats. Biomed Pharmacother 2017; 96: 86-97.
16) Hajji S, Khedir SB, Hamza-Mnif I, Hamdi M, Jedidi I, Kallel R, Boufi S, Nasri M. Biomedical potential of chitosan-silver nanoparticles with special reference to antioxidant, antibacterial, hemolytic and in vivo cutaneous wound healing effects. Biochim Biophys Acta Gen Subj 2019; 1863: 241-254.
17) Yasin S, Liu L, Yao J. Biosynthesis of silver nanoparticles by bamboo leaves extract and their antimicrobial activity. J Fiber Bioeng Inform 2013; 6: 77-84.
18) Yan JK, Cai PF, Cao XQ, Ma HL, Zhang Q, Hu NZ, Zhao YZ. Green synthesis of silver nanoparticles using 4-acetamido-TEMPO-oxidized curdlan. Carbohydr Polym 2013; 97: 391-397.
19) Marimuthu S, Rahuman AA, Rajakumar G, Santhoshkumar T, Kirthi AV, Jayaseelan C, Bagavan A, Zahir AA, Elango G, Kamaraj C. Evaluation of green synthesized silver nanoparticles against parasites. Parasitol Res 2011; 108: 1541-1549.
20) Castro L, Blázquez ML, Muñoz JA, González F, Ballester A. Biological synthesis of metallic nanoparticles using algae. IET Nanobiotechnol 2013; 7: 109-116.
21) Brayner R, Barberousse H, Hemadi M, Djedjat C, Yéprémian C, Coradin T, Livage J, Fiévet F, Couté A. Cyanobacteria as bioreactors for the synthesis of Au, Ag, Pd, and Pt nanoparticles via an enzyme-mediated route. J Nanosci Nanotechnol 2007; 7: 2696-2708.
22) Surwade P, Ghildyal C, Weikel C, Luxton T, Peloquin D, Fan X, Shah V. Augmented antibacterial activity of ampicillin with silver nanoparticles against methicillin-resistant Staphylococcus aureus (MRSA). J Antibiot (Tokyo) 2018; 72: 50-53.
23) Abdel Rahim KA, Ali Mohamed AM. Bactericidal and antibiotic synergistic effect of nanosilver against methicillin-resistant Staphylococcus aureus. Jundishapur J Microbiol 2015; 8: e25867.
24) Labruère R, Sona AJ, Turos E. Anti-methicillin-resistant Staphylococcus aureus nanoantibiotics. Front Pharmacol 2019; 10: 1121.
25) Tian J, Wong KK, Ho CM, Lok CN, Yu WY, Che CM, Chiu JF, Tam PK. Topical delivery of silver nanoparticles promotes wound healing. ChemMedChem 2007; 2: 129-136.
26) Wasef LG, Shaheen HM, El-Sayed YS, Shalaby TIA, Samak DH, Abd El-Hack ME, Al-Owaimer A, Saadeldin IM, El-Mleeh A, Ba-Awadh H, Swelum AA. Effects of silver nanoparticles on burn wound healing in a mouse model. Biol Trace Elem Res 2020; 193: 456-465. doi:10.1007/s12011-019-01729-z.